



# Metalloporphyrins immobilized on montmorillonite as biomimetic catalysts in the oxidation of lignin model compounds

Claudia Crestini\*, Alessandra Pastorini, Pietro Tagliatesta

*Dipartimento di Scienze e Tecnologie Chimiche Università di Tor Vergata, Via della Ricerca Scientifica, 00133 Rome, Italy*

Received 8 April 2003; received in revised form 8 April 2003; accepted 13 July 2003

## Abstract

Biomimetic catalysts such as metalloporphyrins, which can yield highly oxidized metallo-oxo species, have been used as lignin peroxidase models. However, natural porphyrins are unstable under catalytic oxidation conditions due to their self-destruction or to the formation of inactive  $\mu$ -oxo complexes. An alternative approach to the preparation of robust catalysts consists in the immobilization of metalloporphyrins on supports that mimic the polypeptide envelope, which protects the catalytic center of natural enzymes. We report here the use of manganese *meso*-tetrakis(tetramethylpyridinio)porphyrin pentaacetate immobilized on the smectite clay montmorillonite as a suprabiotic catalyst for the oxidation of lignin model compounds.

© 2003 Elsevier B.V. All rights reserved.

**Keywords:** Bioinorganic chemistry; Supported catalysis; Oxidation; Porphyrins; Clays; Biomimetic synthesis

## 1. Introduction

The best characterized lignin degrading fungus is the basidiomycete *Phanerochaete chrisosporium* [1]. In 1983, an extracellular lignin peroxidase (ligninase, LiP) was isolated from ligninolytic cultures of this microorganism [2].

In the presence of hydrogen peroxide, the active center of LiP performs a one-electron oxidation of the lignin aromatic moieties [3]. The catalytic cycle consists in a two electron oxidation of Fe(III) protoporphyrin IX (high spin) to give a highly reactive oxo-iron(IV) protoporphyrin IX  $\pi$ -cation radical, the LiP I complex (LiP compound I) [4,5]. The LiP compound I is then reduced to the initial state by two different one-electron reductions by the substrates [6]. LiP is a fragile enzyme. When exposed to an excess of hydrogen peroxide (more than 20 equivalents), it is subject to inactivation by overoxidation, and gives the inactive form, LiP III [7,8].

Lignin itself can be oxidized by LiP in the presence of limiting amounts of hydrogen peroxide with different degrees of success [9–12]. In principle, the use of an enzymatic system for delignification is not economically convenient with respect to simpler catalysts, due to the costs of purification.

Moreover, since LiP is sensitive to hydrogen peroxide excess, its practical utilization in pulp and paper is difficult to develop. Hence the need for the design of suitable ligninase models resistant to peroxide inactivation. These biomimetic systems are also helpful for the understanding the mechanisms of complex lignin degradation.

Natural metalloporphyrins suffer from the major disadvantage of being unstable in the presence of excess oxidants. Their lability is due either to self-destruction or to the formation of inactive  $\mu$ -oxo complexes [13,14]. The study of biomimetic systems has thus focused toward the development of synthetic metalloporphyrins more resistant to degradative oxidation.

Synthetic metalloporphyrins have been used as biomimetic lignin peroxidase models, and their potentiality for lignin degradation has been a subject of several studies [13–17]. When synthetic metalloporphyrins are used as biomimetic catalysts in the presence of hydrogen peroxide, several side reactions can occur. The peroxidic bond can undergo homolytic scission to yield Fe(IV)-OH and hydroxyl radical in a Fenton like fashion. This reactivity is more significant in the presence of iron complexes and hydrogen peroxide as oxygen donor. A second molecule of peroxide may react with the metal oxo complex in a catalase like fashion to yield the formation of H<sub>2</sub>O and O<sub>2</sub>, and ultimately the degradation of the active oxidant species. The metallo-oxo

\* Corresponding author. Tel.: +39-06-7259-4734; fax: +39-06-7259-4754.

E-mail address: [crestini@uniroma2.it](mailto:crestini@uniroma2.it) (C. Crestini).

complex may further react to yield inactive  $\mu$ -oxo dimers [13].

In Nature, the polypeptidic envelope of the enzyme protects the active site from side reactions, and activates it. The heterolytic cleavage of the peroxidic bond is subject to acid catalysis. The proximal His residue activates the complex to heterolytic cleavage by enhancing the electrophilic character of the oxygen atom, and reducing the strength of the metal-oxygen bond. The manganese porphyrins are not strictly biomimetic systems of LiP, since the natural enzyme active site is an iron complex. However, the use of manganese complexes could override many reactivity problems. More specifically, manganese porphyrins form single adducts with nitrogen bases and in this way can be easily activated. Moreover, manganese shows a smaller tendency than iron to undergo homolytic cleavage of the peroxidic bond. Metalloporphyrins have been considered as possible biomimetic systems for lignin peroxidase [16,17].

Despite the progress achieved in the synthesis of porphyrins resistant to oxidation and in the selection of better conditions suitable for bleaching processes, a major drawback is still present to their applicability. The potential use of metalloporphyrins in lignin oxidation is bound to the possibility of a further increase of their stability toward hydrogen peroxide, and of a possible recovery and recycle of the catalyst after its use. A possible approach to the development of such new catalysts has been attempted taking into consideration that these two aims could be reached by immobilization of the catalyst onto a suitable support. This introduces the possibility to recycle the catalyst and to tune its reactivity by the choice of supports with different immobilization characteristics [16,17].

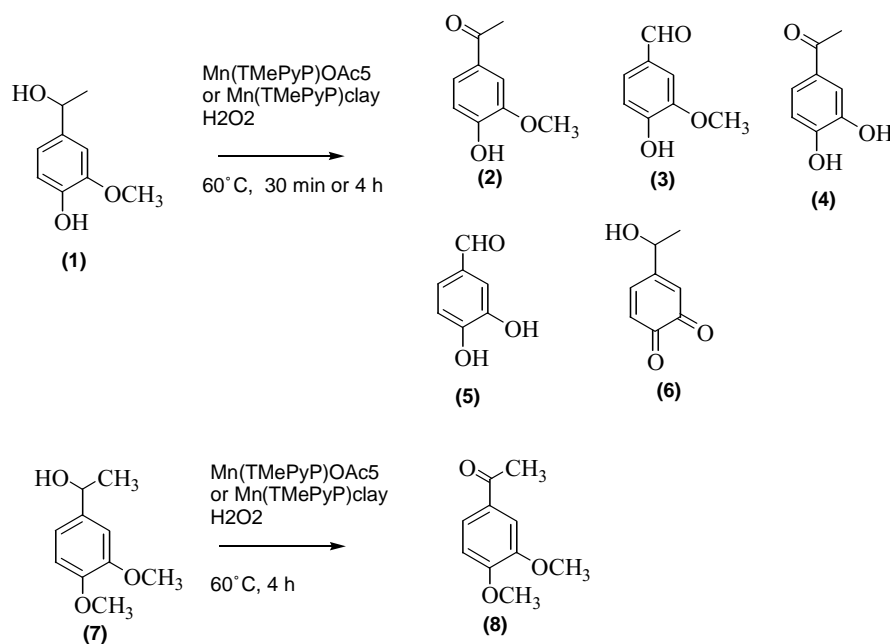
Table 1

Substrate conversion and products yield in the Mn(TMePyP)OAc<sub>5</sub> and Mn(TMePyP)clay catalysed H<sub>2</sub>O<sub>2</sub> oxidation of monomeric lignin models **1** and **7**

Treatment/substrate	Substrate conversion (%)	Products yield (%)					
		<b>2</b>	<b>3</b>	<b>4</b>	<b>5</b>	<b>6</b>	<b>8</b>
Control 30 min/ <b>1</b>	28.8	–	–	–	–	–	–
Mn(TMePyP)OAc <sub>5</sub> 30 min/ <b>1</b>	35.4	tr <sup>a</sup>	–	–	–	–	–
Mn(TMePyP)clay 30 min/ <b>1</b>	39.5	2.6	–	–	–	–	–
Control 4 h/ <b>1</b>	36.9	8.2	8.7	tr	5.9	1.1	–
Mn(TMePyP)OAc <sub>5</sub> 4 h/ <b>1</b>	59.0	4.7	5.6	tr	9.2	1.5	–
Mn(TMePyP)clay 4 h/ <b>1</b>	51.5	1.1	2.0	–	2.3	1.0	–
Control 4 h/ <b>7</b>	22.6	–	–	–	–	–	3.9
Mn(TMePyP)OAc <sub>5</sub> 4 h/ <b>7</b>	24.9	–	–	–	–	–	1.7
Mn(TMePyP)clay 4 h/ <b>7</b>	47.8	–	–	–	–	–	1.0

<sup>a</sup> tr: Trace.

Several approaches of this kind are possible ranging from organic synthetic polymers to biopolymers or to inorganic matrices. Several procedures for their immobilization onto inert matrices have been developed [18]. Smectite clay minerals such as montmorillonite have layer lattice structures in which two-dimensional oxyanions are separated by layers of hydrated cations. The hydrated cations on the interlamellar surfaces of the native minerals can be replaced with almost any desired cation by utilizing simple ion exchange methods [19]. Thus, immobilization onto clays would prevent from the formation of  $\mu$ -oxo dimers. In this case a cationic metalloporphyrin can be immobilized by axial ligation of the metal center with the oxyanions layers, electrostatic



Scheme 1.

interaction between the cationic centers of the porphyrin and the oxyanion moieties, and by physical encapsulation [20].

The cationic manganese *meso*-tetrakis(tetramethylpyridinio)porphyrin pentaacetate supported on montmorillonite Mn(TMePyP)clay revealed to be an efficient catalyst in hydrogen peroxide oxidation reactions [21].

In this effort an array of model compounds resembling the principal bonding pattern of native and residual lignin was selected and its reactivity was studied in the presence of the cationic porphyrin manganese *meso*-tetrakis(tetramethylpyridinio)porphyrin pentaacetate Mn(TMePyP)OAc<sub>5</sub> immobilized onto montmorillonite Mn(TMePyP)clay.

## 2. Results and discussion

As the first lignin model compound the simple phenolic apocinol **1** was chosen. It was reacted in the presence of hydrogen peroxide and Mn(TMePyP)OAc<sub>5</sub> or Mn(TMePyP)clay. The reaction mixtures were studied at different reaction times in order to highlight the early oxidation products obtained. After 30 min reaction time, the only recovered product was the corresponding acetophenone **2** (Scheme 1).

The percentages of substrate conversion show that the model was actively oxidized both in the presence of the soluble and the immobilized catalyst Mn(TMePyP)clay (Table 1). More specifically, in the presence of the supported catalyst the substrate conversion was found even higher than in the presence of the Mn(TMePyP)OAc<sub>5</sub>. The oxidation product isolated arose clearly from a side-chain oxidation process. When the reaction time was increased at 4 h, the substrate conversions were found enhanced at 59.0 and 51.5%, respectively (Table 1).

These data indicate that the immobilized catalyst retains its activity even after several hours. In the latter case also other oxidation products were identified and characterized as shown in Scheme 1. Vanillin **3** is a product of side-chain cleavage; compounds **4** and **5** are demethylation and side-chain-oxidation products, while the *o*-quinone **6** was formed by oxidation at the C-3 of the aromatic ring.

This reactivity pattern is in accord with the previously reported for both lignin peroxidase and metalloporphyrins. Thus, Mn(TMePyP)clay is an efficient biomimetic system of LiP.

Our attention was next turned to the reactivity of the corresponding non-phenolic lignin model compound 1(3,4-dimethoxyphenyl)-1-ethanol **7**. Since non-phenolic compounds are usually less reactive than the corresponding phenolic ones, only a reaction time of 4 h was considered. When the oxidation reaction was carried out on **7**, a different reaction pattern was revealed (Scheme 1). The only recovered oxidation product was the corresponding acetophenone **8**, the product of side-chain oxidation. Also in this case the percentages of conversion of the substrate showed that both the catalysts were active even though the reactivity was lower in the case of the supported catalyst (Table 1).

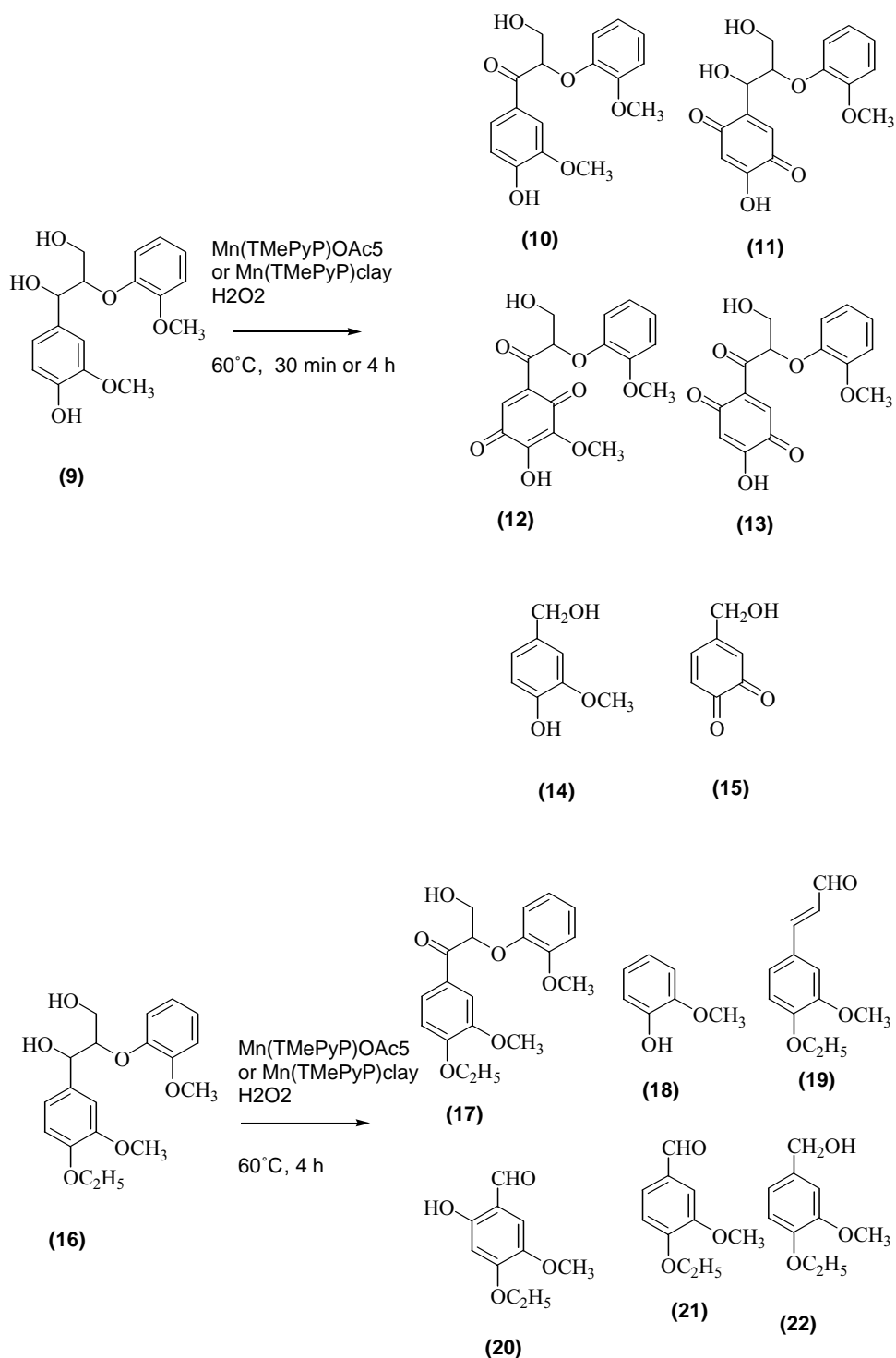
Once clarified the reactivity of monomeric lignin-like sub-units, our attention was focused on the behavior of  $\beta$ -O-4 arylglycerol-phenyl ethers, that represent the most abundant lignin interunit linkage. For this purpose both a phenolic and non-phenolic models were synthesized. The phenolic model compound **9** reacted in the presence of both the soluble and immobilized manganese porphyrin, showing that the catalytic activity is retained by Mn(TMePyP)clay even in the presence of bulky molecules (Scheme 2).

When the soluble catalyst Mn(TMePyP)OAc<sub>5</sub> was used, after 30 min of reaction several products of oxidation were identified (Table 2). More specifically they are products of side-chain oxidation **10**, *p*-quinone formation, **11**, side-chain oxidation and quinone formation **12** and **13**, and products of side-chain cleavage **14**, and side-chain cleavage and *o*-quinone formation **15** (Table 2). In the presence of the immobilized catalyst only **11** and **14** were recovered after 30 min. When the reaction was carried out during 4 h, besides the expected increase of the conversion amount, in the presence of the heterogeneous catalyst compounds **11**, **13**, **14** and **15** were identified. Since the mass balance is not quantitative this indicates that the substrates give rise to the formation of polymeric products and/or water soluble low molecular weight fragments that cannot be evidenced by the technique used in this effort. However, the phenolic  $\beta$ -O-4 model compound **9** was extensively oxidized under

Table 2  
Substrate conversion and products yield in the Mn(TMePyP)OAc<sub>5</sub> and Mn(TMePyP)clay catalysed H<sub>2</sub>O<sub>2</sub> oxidation of  $\beta$ -O-4 lignin models **9** and **16**

Treatment/substrate	Substrate conversion (%)	Products yield (%)											
		<b>10</b>	<b>11</b>	<b>12</b>	<b>13</b>	<b>14</b>	<b>15</b>	<b>17</b>	<b>18</b>	<b>19</b>	<b>20</b>	<b>21</b>	<b>22</b>
Control 30 min/ <b>9</b>	24.3	–	9.4	–	2.2	–	tr <sup>a</sup>						
Mn(TMePyP)OAc <sub>5</sub> 30 min/ <b>9</b>	44.7	7.3	10.2	13.3	7.8	tr <sup>a</sup>	tr <sup>a</sup>						
Mn(TMePyP)clay 30 min/ <b>9</b>	41.1	–	9.8	–	–	tr <sup>a</sup>	–						
Control 4 h/ <b>9</b>	28.8	tr <sup>a</sup>	9.6	tr <sup>a</sup>	4.8	tr <sup>a</sup>	tr <sup>a</sup>						
Mn(TMePyP)OAc <sub>5</sub> 4 h/ <b>9</b>	59.6	5.3	5.2	12.5	4.9	tr <sup>a</sup>	tr <sup>a</sup>						
Mn(TMePyP)clay 4 h/ <b>9</b>	52.9	–	4.5	–	5.4	tr <sup>a</sup>	tr <sup>a</sup>						
Control 4 h/ <b>16</b>	61.2							1.5	4.4	5.9	1.7	tr <sup>a</sup>	–
Mn(TMePyP)OAc <sub>5</sub> 4 h/ <b>16</b>	81.0							1.7	2.4	3.1	1.3	tr <sup>a</sup>	tr <sup>a</sup>
Mn(TMePyP)clay 4 h/ <b>16</b>	80.4							1.0	4.2	3.5	1.6	tr <sup>a</sup>	tr <sup>a</sup>

<sup>a</sup> tr: Trace.

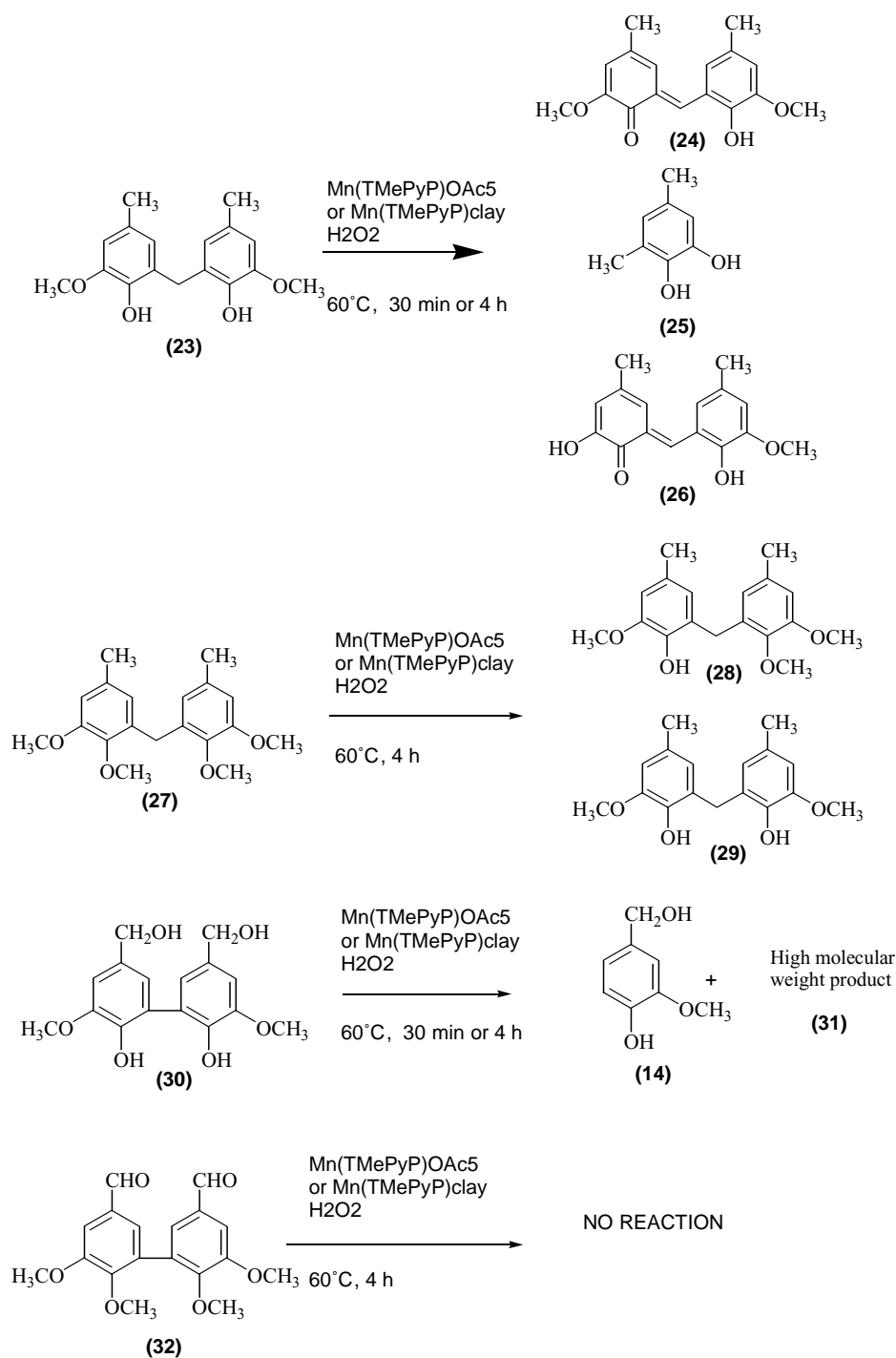


Scheme 2.

both the experimental conditions. The corresponding non-phenolic model **16** when oxidized with both the soluble and immobilized metalloporphyrin showed an interesting reactivity (Scheme 2). The conversion amount was comparable in the two cases (Table 2) and the oxidation products recovered, **17–22** are all products of side-chain oxidation or cleavage (Scheme 2). The presence of the aldehyde

**20** indicates that non-phenolic aromatic rings can also be hydroxylated.

During lignin oxidation, the interunit linkages are modified with the formation of condensed structures such as diphenyl methanes and biphenyls. Such condensed subunits are generally more recalcitrant to oxidation than the native lignin interunit bonding. In order to explore the reactivity



Scheme 3.

of our catalysts toward such structures we synthesized two different diphenylmethane and two different biphenyl model compounds. The phenolic diphenyl methane **23** was found to be degraded at a considerable extent after 30 min yielding to the formation of the semiquinone **24** and to the product of side-chain cleavage **25** (Scheme 3).

When the reaction was carried out during 4 h also the semiquinone **26**, a product of demethylation of the alkyl-aryl

ether moiety was found. In both cases the reactivity of the soluble and heterogeneous catalyst  $\text{Mn(TMePyP)OAc}_5$  and  $\text{Mn(TMePyP)clay}$  were comparable (Table 3). The non-phenolic diphenylmethane model **27** was found also reactive in the presence of hydrogen peroxide and  $\text{Mn(TMePyP)OAc}_5$  or  $\text{Mn(TMePyP)clay}$  (Scheme 3). However, only low amounts of demethylation products **28** and **29** were detected. Also in this case the mass balance shows

Table 3

Substrate conversion and products yield in the Mn(TMePyP)OAc<sub>5</sub> and Mn(TMePyP)clay catalysed H<sub>2</sub>O<sub>2</sub> oxidation of diphenylmethane lignin models **23** and **27**

Treatment/substrate	Substrate conversion (%)	Products yield				
		<b>24</b>	<b>25</b>	<b>26</b>	<b>28</b>	<b>29</b>
Control 30 min/ <b>23</b>	21.1	–	1.0			
Mn(TMePyP)OAc <sub>5</sub> 30 min/ <b>23</b>	24.7	11.0	tr <sup>a</sup>			
Mn(TMePyP)clay 30 min/ <b>23</b>	23.4	1.4	1.1			
Control 4 h/ <b>23</b>	27.6	–	1.0	1.0		
Mn(TMePyP)OAc <sub>5</sub> 4 h/ <b>23</b>	38.9	11.3	tr <sup>a</sup>	tr <sup>a</sup>		
Mn(TMePyP)clay 4 h/ <b>23</b>	38.7	2.5	1.0	1.0		
Control 4 h/ <b>27</b>	46.9				tr <sup>a</sup>	tr <sup>a</sup>
Mn(TMePyP)OAc <sub>5</sub> 4 h/ <b>27</b>	48.2				1.1	tr <sup>a</sup>
Mn(TMePyP)clay 4 h/ <b>27</b>	46.8				tr <sup>a</sup>	tr <sup>a</sup>

<sup>a</sup> tr: Trace.

Table 4

Substrate conversion and products yield in the Mn(TMePyP)OAc<sub>5</sub> and Mn(TMePyP)Clay catalysed H<sub>2</sub>O<sub>2</sub> oxidation of biphenyl lignin model **30**

Treatment/substrate	Substrate conversion (%)	Products yield (%)	
		<b>14</b>	<b>31</b>
Control 30 min/ <b>30</b>	53.4	tr <sup>a</sup>	–
Mn(TMePyP)OAc <sub>5</sub> 30 min/ <b>30</b>	85.4	tr <sup>a</sup>	1.1
Mn(TMePyP)clay 30 min/ <b>30</b>	80.6	tr <sup>a</sup>	–
Control 4 h/ <b>30</b>	79.8	tr <sup>a</sup>	–
Mn(TMePyP)OAc <sub>5</sub> 4 h/ <b>30</b>	93.2	tr <sup>a</sup>	1.2
Mn(TMePyP)clay 4 h/ <b>30</b>	81.1	tr <sup>a</sup>	–

<sup>a</sup> tr: Trace.

that products of polymerization, and/or fragmentation to low molecular weight water soluble compounds are formed that cannot be detected.

On the other hand, the biphenyl phenolic model **30** (Scheme 3) was extensively oxidized. Also in this case the reactivity of the two catalysts is comparable (Table 4).

The oxidation products recovered are the vanillic alcohol **14**, a product of side-chain cleavage, and a product at high molecular weight (>550), probably a tetramer. On the contrary, the non-phenolic biphenyl model **32** was not reactive under our experimental conditions. The recovery of products **14** and **25** in the oxidation of **30** and **23**, respectively, indicates that phenolic condensed lignin subunits can be oxidized with cleavage of the side-chain by Mn(TMePyP)OAc<sub>5</sub> and Mn(TMePyP)clay (Scheme 3).

### 3. Conclusion

Mn(TMePyP)clay is an efficient immobilized catalyst for the hydrogen peroxide oxidation of monomeric and dimeric lignin model compounds. It is able to oxidize both phenolic and non-phenolic models, with the formation of products of side-chain oxidation and cleavage. This behavior implies a

potential delignification effect in view of the possibility to depolymerize lignin. Several products of aromatic ring hydroxylation or demethylation of the alkyl-aryl ether moiety were also characterized. This indicates a potential reactivity of aromatic ring cleavage. Condensed phenolic model compounds showed also to be reactive under these experimental conditions. This is an important prerequisite for an efficient delignification process. This reactivity pattern makes Mn(TMePyP)clay an ideal candidate for the study and development of alternative delignification procedures since it constitutes an efficient and potentially recyclable catalyst for effective degradation of lignin model compounds.

### 4. Experimental

<sup>1</sup>H and <sup>13</sup>C NMR spectra were recorded on a Bruker AM 400 spectrometer. Mass Spectroscopy (MS) was performed with a GC Shimadzu GC-17A and a mass-selective detector QP 6000. All solvents were ACS reagent grade and were redistilled and dried according to standard procedures. Chromatographic purifications were performed on columns packed with Merck silica gel 60, 230–400 mesh for flash technique. Thin layer chromatography was carried out using Merck platten Kieselgel 60 F254.

Lignin model compounds **1**, **7**, **9**, **16**, **23**, **27**, **30** and **32** were synthesized according to literature procedures [21–23].

#### 4.1. Catalysts preparation

The manganese porphyrin Mn(TMePyP)OAc<sub>5</sub> was synthesized according to literature procedures [24]. Mn(TMePyP)OAc<sub>5</sub> was immobilized on montmorillonite as previously reported by refluxing in the presence of Na<sup>+</sup> saturated montmorillonite [20].

#### 4.2. Typical procedure for the oxidation of lignin model compounds

Hydrogen peroxide (10%) was added with stirring at 60 °C at 20 μl aliquots every 1 h to a solution of the porphyrin catalyst (1 mg) in 0.5 ml of dioxane/buffer citrate phosphate 100 mM pH 6 containing 50 μmol of substrate. After 4 h the reaction mixtures were extracted in CH<sub>2</sub>Cl<sub>2</sub> in the presence of saturated aqueous NaCl solution. The organic layer was dried over MgSO<sub>4</sub> and evaporated under reduced pressure. The residues were dissolved in 20 μl of pyridine in the presence of 3,4-dimethoxytoluene as an internal standard for GC-MS analysis. The mixture was then silylated by addition of bis-trimethylsilyl trifluoroacetamide (BSTFA).

#### 4.3. Characterization of products

Gas chromatography and gas chromatography–mass spectrometry of the reaction products were performed using a



Table 5  
Mass spectrometric data

Product	Derivative <sup>a</sup>	MS ( <i>m/z</i> ) data (%)
2	–Si(CH <sub>3</sub> ) <sub>3</sub>	238 ( <i>M</i> <sup>+</sup> , 41), 223 (35), 209 (9), 193 (23), 91 (10), 73 (100)
3	–Si(CH <sub>3</sub> ) <sub>3</sub>	MS (%): 224 ( <i>M</i> <sup>+</sup> , 45), 209 (15), 193 (22), 177 (5), 137 (8), 73 (100)
4	–Si(CH <sub>3</sub> ) <sub>3</sub>	224 ( <i>M</i> <sup>+</sup> , 18), 209 (10), 193 (15), 179 (31), 151 (9), 73 (100)
5	–Si(CH <sub>3</sub> ) <sub>3</sub>	296 ( <i>M</i> <sup>+</sup> , 8), 224 (30), 209 (10), 193 (23), 151(84), 73 (100)
6	–Si(CH <sub>3</sub> ) <sub>3</sub>	282 ( <i>M</i> <sup>+</sup> , 8), 223 (40), 207 (6), 192 (35), 177 (6), 73 (100)
7	–	182 ( <i>M</i> <sup>+</sup> , 42), 167 (64), 139 (100), 124 (30), 108 (21), 77 (45)
8	–	180 ( <i>M</i> <sup>+</sup> , 45), 165 (100), 137 (17), 122 (10), 107 (8), 77 (26)
10	–Si(CH <sub>3</sub> ) <sub>3</sub>	224 (15), 209 (10), 194 (5), 166 (12), 150 (76), 73 (100)
11	–Si(CH <sub>3</sub> ) <sub>3</sub>	297 (12), 223 (5), 181 (5), 166 (6), 109 (8), 73 (100)
12	–Si(CH <sub>3</sub> ) <sub>3</sub>	252 (9), 209 (5), 166 (8), 124 (7), 103 (12), 73 (100)
13	–Si(CH <sub>3</sub> ) <sub>3</sub>	224 (9), 209 (6), 194 (8), 166 (10), 150 (45), 73 (100)
14	–Si(CH <sub>3</sub> ) <sub>3</sub>	298 ( <i>M</i> <sup>+</sup> , 13), 283 (6), 268 (9), 209 (9), 179 (6), 73 (100)
15	–Si(CH <sub>3</sub> ) <sub>3</sub>	210 ( <i>M</i> <sup>+</sup> , 12), 179 (18), 136 (20), 147 (10), 105 (8), 73 (100)
16	–	330 ( <i>M</i> <sup>+</sup> -18, 16), 206 (17), 179 (26), 151 (33), 109 (47), 77 (100)
17	–	328 ( <i>M</i> <sup>+</sup> -18, 17), 207 (35), 179 (100), 151 (63), 137 (7), 123 (21)
18	–	124 ( <i>M</i> <sup>+</sup> , 65), 109 (100), 81 (89), 65 (15), 77 (21), 53 (55)
19	–	206 ( <i>M</i> <sup>+</sup> , 33), 179 (8), 151 (100), 123 (18), 77 (24), 55 (90)
20	–	196 ( <i>M</i> <sup>+</sup> , 22), 181 (37), 153 (30), 135 (33), 125 (51), 93 (100)
21	–	180 ( <i>M</i> <sup>+</sup> , 37), 151 (100), 109 (17), 95 (10), 81 (20), 65 (25)
22	–	180 ( <i>M</i> <sup>+</sup> , 50), 154 (38), 137 (40), 122 (48), 109 (21), 65 (100)
23	–Si(CH <sub>3</sub> ) <sub>3</sub>	432 ( <i>M</i> <sup>+</sup> , 38), 417 (24), 402 (26), 329 (8), 73 (100)
24	–Si(CH <sub>3</sub> ) <sub>3</sub>	358 ( <i>M</i> <sup>+</sup> , 5), 344 (6), 268 (5), 180 (4), 103 (10), 73 (100)
25	–Si(CH <sub>3</sub> ) <sub>3</sub>	282 ( <i>I</i> <sup>+</sup> , 9), 267 (8), 252 (7), 193 (8), 150 (30), 73 (100)
26	–Si(CH <sub>3</sub> ) <sub>3</sub>	344 ( <i>M</i> <sup>+</sup> , 4), 268 (5), 180 (14), 103 (13), 91 (8), 73 (100)
27	–	316 ( <i>M</i> <sup>+</sup> , 49), 165 (30), 151 (100), 135 (90), 127 (13), 77 (18)
28	–Si(CH <sub>3</sub> ) <sub>3</sub>	374( <i>M</i> <sup>+</sup> , 52), 344(72), 313 (18), 193 (31), 151(32), 73 (100)
29	–Si(CH <sub>3</sub> ) <sub>3</sub>	432 ( <i>M</i> <sup>+</sup> , 38), 417 (24), 402 (26), 329 (8), 73 (100)
31	–Si(CH <sub>3</sub> ) <sub>3</sub>	344 (8), 209 (4), 165 (5), 133 (5), 89 (7), 73 (100)

<sup>a</sup> Underivatized; –Si(CH<sub>3</sub>)<sub>3</sub>: trimethylsilylated with *N,O*-(trimethylsilyl)-acetamide.

DB1 column (30 m × 0.25 mm and 0.25 mm film thickness), and an isothermal temperature profile of 100 °C for the first two min, followed by a 20 °C/min temperature gradient to 300 °C and finally an isothermal period at 300 °C for 10 min. The injector temperature was 280 °C. Chromatography grade helium was used as the carrier gas. The identification of **2–5**, **8**, **10**, **14**, **17**, **18**, **19**, **21**, **22**, **25** was carried out by comparison with sample of authentic products, **6**, **15**, **20**, **28**, **29** were assigned by comparison with the fragmentation spectra of original compounds. Products **11–13**, **24**, **26**, **31** were tentatively identified on the basis of the fragmentation spectra. The fragmentation patterns are shown in Table 5.

## Acknowledgements

Italian M.U.R.S.T. and C.N.R. are acknowledged for financial support.

## References

- [1] M. Tien, T.K. Kirk, Science 221 (1983) 661.
- [2] J.K. Glenn, M.A. Morgan, M.B. Mayfield, M. Kuwahara, M.H. Gold, Biochem. Biophys. Res. Commun. 114 (1983) 1077.
- [3] T.K. Kirk, R.L. Farrell, Annu. Rev. Microbiol. 41 (1987) 465–505.
- [4] B. Chance, Arch. Biochem. Biophys. 41 (1952) 416–424.
- [5] A. Khindaria, S.D. Aust, Biochemistry 35 (1996) 13107–13111.
- [6] R.S. Koduri, M. Tien, Biochemistry 33 (1994) 4225–4230, and references cited therein.
- [7] H. Wariishi, M.H. Gold, FEBS Lett. 243 (1989) 165–168.
- [8] H. Wariishi, M.H. Gold, J. Biol. Chem. 265 (1990) 2070–2077.
- [9] B. Kurek, B. Monties, Enzyme Microb. Technol. 16 (1994) 125–130.
- [10] K.E. Hammel, M.A. Moen, Enzyme Microb. Technol. 13 (1991) 15–18.
- [11] H. Wariishi, K. Valli, M.H. Gold, Biochem. Biophys. Res. Commun. 176 (1991) 269–275.
- [12] K.E. Hammel, K.A. Jensen, M.D. Mozuch, L.L. Landucci, M. Tien, E.A. Pease, J. Biol. Chem. 268 (1993) 12274–12281.
- [13] R.A. Sheldon (Ed.), Metalloporphyrins in Catalytic Oxidations, Marcel Dekker Inc., New York, 1994.
- [14] B. Meunier, Metalloporphyrins Catalyzed Oxidations, in: F. Montanari, L. Casella (Eds.), Kluwer Academic Publishers, Dordrecht, 1994, pp. 11–19.
- [15] C. Crestini, R. Saladino, P. Tagliatesta, T. Boschi, Bioorg. Med. Chem. 7 (1999) 1897.
- [16] C. Crestini, D.S. Argyropoulos, in: D.S. Argyropoulos (Ed.), Oxidative Delignification Chemistry, ACS Symposium Series 397, Washington, DC, 1989, pp. 373–390.
- [17] C. Crestini, P. Tagliatesta, in: K.M. Kadish, K.M. Smith, R. Guilard (Eds.), The Porphyrin Handbook II, vol. 11, Academic Press, Chapter 66, in press.
- [18] G. Labat, B.J. Meunier, J. Org. Chem. 54 (1989) 5008–5011.
- [19] T.J. Pinnavaia, Science 220 (1983) 3659.

- [20] L. Barloy, P. Battioni, D.J. Mansuy, *J. Chem. Soc. Chem. Commun.* (1990) 1365.
- [21] C. Crestini, M. D'Auria, *Tetrahedron* 53 (1997) 7877.
- [22] H. Xu, S. Omori, Y.-Z. Lai, *Holzforschung* 49 (1995) 323.
- [23] M.G. Drumond, D. Pilò Veloso, S.D. Santos Cota, S.A. Lemos de Morais, E.A. do Nascimento, C. Cheng, *Holzforschung* 46 (1992) 127.
- [24] J. Bernadou, G. Pratviel, F. Bennis, M. Girardet, B. Meunier, *Biochemistry* 28 (1989) 7268.